Pergamon

Int. J. Heat Mass Transfer. Vol. 41, No. 13, pp. 1917–1928, 1998

Printed in Great Britain
0017-9310/98 $19.00 + 0.00

PII: S0017-9310(97)00313-X

The natural convection of liquid metal in a cubical enclosure with various electro-conductivities of the wall under the magnetic field

TOSHIO TAGAWA† and HIROYUKI OZOE‡
Institute of Advanced Material Study, Kyushu University, Kasuga 816, Japan

(*Received* 11 *October* 1997)

Abstract—The natural convection of liquid metal in a cubical enclosure was numerically studied for various electro-conductivities of the wall from zero to infinity under a static magnetic field. The cubical enclosure was heated from one vertical wall and cooled from an opposing vertical wall both isothermally and four other walls were thermally insulated. The direction of the static magnetic field was perpendicular to the heated and cooled walls (X-direction) or parallel to the heated and cooled walls (Y-direction) for the present work. All calculations were carried out for the Rayleigh number 10^5, the Prandtl number 0.025, and the Hartmann number 100. Under the X-directional magnetic field, the average heat transfer rate was effectively suppressed with an increase in the electro-conductivity of the wall. Under the Y-directional magnetic field, the average heat transfer rate was only slightly suppressed for the electrically insulated wall, but drastically decreased with an increase in the electro-conductivity of the wall.

1. INTRODUCTION

The recent development of technology requires to treat the electro-conductive fluid such as liquid metal as a working medium. Some of the practical application systems include the magnetohydrodynamic power generation system, high speed ship driven by super conductive magnetic system, cooling medium for nuclear reactor with a magnetic driven pumping system, continuous steel casting system magnetically agitated or suppressed and crystallization of molten semiconducting material with magnetically suppressed or driven system.

The flow of these fluids is sometimes controlled by the application of a magnetic field with using of the electro-conductive characteristics of the fluid. These operating fluids are more or less in contact with the surrounding vessels and/or conduits, whose electro-conductivity would affect the flow characteristics furthermore under an external magnetic field. It is the motivation to clarify the effect of the electro-conductivities of the wall on the natural convection of liquid metal.

Recently, Ozoe and Okada [1] numerically studied the effect of the direction of external magnetic fields on the natural convection of liquid metal in a cubical enclosure. They found that the effect of magnetic suppression was quite different depending on the direction of the magnetic field. They then carried out the experiments with liquid gallium [2] and confirmed their numerical prediction. However, their study was confined to the electrically insulated walls. The same problem for the perfectly electro-conducting walls with the deletion of electric field term from the Ohm's law was investigated numerically by Tagawa and Ozoe [3]. The magnetic suppression for the perfectly electro-conducting walls was much stronger than that for the electrically insulated walls. Their result motivated to study the effect of electro-conductivity of the wall in general. This paper treats the electro-conductivity of the walls from zero to infinity for the natural convection of liquid metal under external magnetic fields. The cubic enclosure was selected to study the present issue in general. The cylinder vessel may be selected for a Czochralski system in a semiconducting industry. However, the mixed convection in a modeled cylinder regime is rather complicated for a study of wall electro-conductivity.

2. THE SYSTEM AND MODEL EQUATIONS

The modeled system is a cubical enclosure as shown in Fig. 1. The cubical enclosure is filled with liquid gallium ($Pr = 0.025$). It is heated from one vertical side wall and cooled from the opposing vertical wall isothermally. Four other walls are thermally insulated. The external magnetic field is either in the X- or Y-directions as shown in Fig. 1. The thickness of the

† Current address: Interdisciplinary Graduate School of Engineering Science, Kyushu University, Kasuga 816, Japan.
‡ Author to whom correspondence should be addressed. Tel.: 81 92583 7834. Fax: 81 92583 7838.

NOMENCLATURE

$\mathbf{b}$	magnetic flux density [T]
b_0	uniform external magnetic flux density [T]
$\mathbf{B}$	dimensionless magnetic flux density $= \mathbf{b}/b_0$ [-]
Cm	electro-conductivity ratio $= \sigma_w/\sigma$ [-]
c_p	specific heat of fluid [J (kg·K)$^{-1}$]
$\mathbf{e}$	electric field [V m^{-1}]
e_0	$= u_0 b_0$ [V m^{-1}]
$\mathbf{E}$	dimensionless electric field $= \mathbf{e}/e_0$ [-]
$\boldsymbol{g}$	acceleration due to gravity [m s^{-2}]
Gr	Grashof number $= \boldsymbol{g}\beta(\theta_h-\theta_c)l^3/\nu^2$ [-]
Ha	Hartmann number $= (\sigma/\mu)^{1/2} b_0 l$ [-]
$\mathbf{j}$	electric current density [A m^{-2}]
j_0	$= \sigma u_0 b_0$ [A m^{-2}]
$\mathbf{J}$	dimensionless electric current density $= \mathbf{j}/j_0$ [-]
l	distance between hot and cold walls [m]
L	l/x_0 [-]
Nu	Nusselt number $= Q_{conv}/Q_{cond}$ [-]
p	pressure [Pa]
p_0	$\rho\alpha^2/x_0^2$ [Pa]
P	dimensionless pressure $= p/p_0$ [-]
Pr	Prandtl number $= \nu/\alpha$ [-]
Q_{cond}	conduction heat flux [J (m^2·s)$^{-1}$]
Q_{conv}	total heat flux [J (m^2·s)$^{-1}$]
Ra	Rayleigh number $= \boldsymbol{g}\beta(\theta_h-\theta_c)l^3/(\alpha\nu) = Gr\cdot Pr$ [-]
t	time [s]
t_0	$= x_0^2/\alpha$ [s]
T	dimensionless temperature $= (\theta-\theta_0)/(\theta_h-\theta_c)$ [-]
T_{cond}	conductive temperature [-]
T_{conv}	convective temperature [-]
$\mathbf{u}$	velocity (u, v, w) [m s^{-1}]
u_0	$= v_0 = w_0 = \alpha/x_0$ [m s^{-1}]
$\mathbf{U}$	dimensionless velocity $(U, V, W) = \mathbf{u}/u_0$ [-]
x	coordinate [m]
x_0	$Ra^{-1/3} l$ [m]
X	x/x_0 [-]
y	coordinate [m]
y_0	$Ra^{-1/3} l$ [m]
Y	y/y_0 [-]
z	coordinate [m]
z_0	$Ra^{-1/3} l$ [m]
Z	z/z_0 [-].

Greek symbols

α	thermal diffusivity of fluid $= \lambda/(\rho c_p)$ [m^2 s^{-1}]
β	volumetric coefficient of expansion [K^{-1}]
θ	temperature [K]
θ_c	cold wall temperature [K]
θ_h	hot wall temperature [K]
θ_0	$= (\theta_h+\theta_c)/2$ [K]
λ	thermal conductivity of fluid [W (m·K)$^{-1}$]
μ	viscosity of fluid [Pa·s]
ν	kinematic viscosity of fluid $= \mu/\rho$ [m^2 s^{-1}]
ρ	density of fluid [kg m^{-3}]
σ	electro-conductivity of fluid [(Ω·m)$^{-1}$]
σ_w	electro-conductivity of wall [(Ω·m)$^{-1}$]
τ	dimensionless time $= t/t_0$ [-]
Φ	dimensionless temperature deviation, see equation (3) [-]
ψ_e	electric scalar potential [V]
ψ_{e0}	$= \alpha b_0$ [V]
Ψ_e	dimensionless electric scalar potential $= \psi_e/\psi_{e0}$ [-].

Operators

∇	$= \mathbf{i}\,\partial/\partial X + \mathbf{j}\,\partial/\partial Y + \mathbf{k}\,\partial/\partial Z$
∇^2	$= \partial^2/\partial X^2 + \partial^2/\partial Y^2 + \partial^2/\partial Z^2$.

surrounding walls is assumed to be 9.62% of the cube length as a representative case. The model equations for natural convection under the external magnetic field consist of continuity, energy and three-directional momentum equations including the Lorentz force terms. The fluid is an incompressible Newtonian fluid with Boussinesq approximation. Electric current density induced by the liquid motion under the external magnetic field is so slight that the magnetic field induced by the electric current density is assumed to be negligible in comparison with the external magnetic field. Joule heating is also negligible in the energy equation. Ohm's law and the conservation of electric current density are both considered. In such a system the model equations become in dimensionless form as follows.

$$\nabla\cdot\mathbf{U} = 0 \tag{1}$$

$$\frac{D\mathbf{U}}{D\tau} = -\nabla P + Pr\,\nabla^2\mathbf{U} + Ha^2\,Pr\,Ra^{-2/3}(\mathbf{J}\times\mathbf{B}) + [0, 0, Pr(\Phi - X/L + 0.5)]^T \tag{2}$$

$$\frac{D\Phi}{D\tau} = \nabla^2\Phi + U/L, \quad \Phi = T - 0.5 + X/L \tag{3}$$

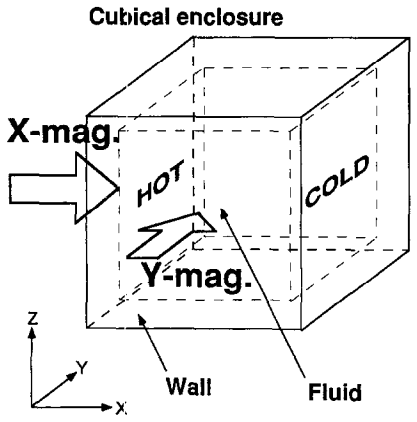

Fig. 1. Schematic of the system.

$$\mathbf{J} = \mathbf{E} + \mathbf{U} \times \mathbf{B} = -\nabla \Psi_e + \mathbf{U} \times \mathbf{B} \quad \text{(fluid)} \tag{4}$$

$$\mathbf{J} = Cm\mathbf{E} = Cm(-\nabla \Psi_e) \quad \text{(wall)} \tag{5}$$

$$\nabla \cdot \mathbf{J} = 0. \tag{6}$$

The dimensionless variables are defined as follows:

$$X = x/x_0, \quad Y = y/y_0, \quad Z = z/z_0, \quad U = u/u_0,$$

$$V = v/v_0, \quad W = w/w_0 \quad P = p/p_0, \quad \tau = t/t_0,$$

$$L = l/x_0 = Ra^{1/3}, \quad T = (\theta - \theta_0)/(\theta_h - \theta_c),$$

$$\Phi = T - 0.5 + X/L, \quad \mathbf{B} = \mathbf{b}/b_0, \quad \mathbf{E} = \mathbf{e}/e_0, \quad \mathbf{J} = \mathbf{j}/j_0,$$

$$\Psi_e = \psi_e/\psi_{e0}, \quad Pr = \nu/\alpha, \quad Ra = g\beta(\theta_h - \theta_c)l^3/(\alpha\nu),$$

$$Ha = (\sigma/\mu)^{1/2} b_0 l, \quad Cm = \sigma_w/\sigma,$$

$$x_0 = y_0 = z_0 = Ra^{-1/3}\, l, \quad t_0 = x_0^2/\alpha,$$

$$u_0 = v_0 = w_0 = \alpha/x_0, \quad \theta_0 = (\theta_h + \theta_c)/2,$$

$$e_0 = u_0 b_0, \quad j_0 = \sigma u_0 b_0,$$

$$\psi_{e0} = \alpha b_0, \quad p_0 = \rho\alpha^2/x_0^2.$$

3. COMPUTATIONAL METHOD

The above simultaneous equations were approximated by the finite difference equations for the non-uniform grid systems. Continuity equation was satisfied for the staggered grid systems for which scalar points (pressure, temperature and electric potential) and vector points (velocity, electric current density and magnetic flux density) were defined at different points, respectively, and pressure was solved by HSMAC method [4]. In the same way, both electric potential and electric current density were solved by the HSMAC method, i.e., electric potential ψ_e and electric current density $\mathbf{J}$ were calculated to satisfy equations (4) and (6) for the fluid regime, or equations (5) and (6) for the wall regime. This electric current density satisfies the conservation of electric charge equation. Inertial terms in the momentum and the energy equations were approximated by the hybrid scheme [5].

Table 1. The grid locations in the half regime. The other half is symmetric in terms of the center plane. The grid locations are the same in the X-, Y- and Z-directions

Region	Point	Grid coordinate
Outer boundary	1	−0.09622
Wall	2	−0.06472
	3	−0.04107
	4	−0.02332
	5	−0.01000
Inner boundary	6	0.00000
Fluid	7	0.01000
	8	0.02332
	9	0.04107
	10	0.06472
	11	0.09622
	12	0.13818
	13	0.19409
	14	0.26857
	15	0.36780
	16	0.50000

The computational grid locations in the X-, Y-, and Z-directions are listed in Table 1. Many grids were clustered near the interface between the wall and fluid. The number of grids in the fluid regime is the same as the previous ref. [3].

4. INITIAL AND BOUNDARY CONDITIONS

The initial condition for the computation of natural convection is a conduction temperature profile and the fluid is stagnant as follows:

$$U = V = W = 0$$

$$\Phi = T - 0.5 + X/L = 0 \quad (T = 0.5 - X/L).$$

The initial condition for the computation of magnetic natural convection is the result obtained from that of the non-magnetic natural convection. The external magnetic field was then applied abruptly. The initial conditions for the electric current density and electric potential are as follows:

$$J_x = J_y = J_z = 0$$

$$\Psi_e = 0.$$

The boundary conditions for velocity and temperature are given as follows:

$$U = V = W = 0 \quad \text{at } X = 0, L,$$

$$Y = 0, L \quad \text{and} \quad Z = 0, L$$

$$\Phi = 0 \quad \text{at } X = 0, L$$

$$\frac{\partial \Phi}{\partial Y} = 0 \quad \text{at } Y = 0, L$$

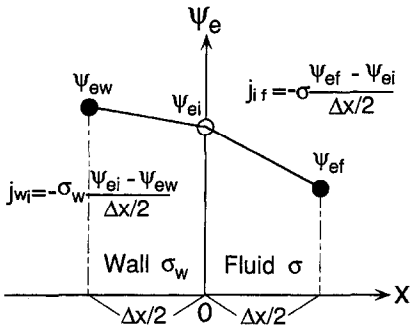

Fig. 2. Electric current density at the interface between the wall and the fluid.

$$\frac{\partial \Phi}{\partial Z} = 0 \quad \text{at } Z = 0, L.$$

The boundary condition for electric current density is presented in Fig. 2. Since the velocity near the solid wall is negligible, the electric current in the fluid is approximated as follows from Ohm's law:

$$j_{if} = -\sigma \frac{\psi_{ef} - \psi_{ei}}{\Delta x/2}.$$

The electric current in the wall is also approximated as follows:

$$j_{wi} = -\sigma_w \frac{\psi_{ei} - \psi_{ew}}{\Delta x/2}.$$

Since the electric current density in the fluid is equal to that in the wall, the electric current at the interface satisfies,

$$j_i = j_{if} = j_{wi} = -\frac{2\sigma\sigma_w}{\sigma + \sigma_w} \frac{\psi_{ef} - \psi_{ew}}{\Delta x}. \tag{7}$$

Hence, the boundary conditions for the dimensionless electric current density at the interface are obtained as follows:

$$J_x = -\frac{2Cm}{1+Cm} \frac{\partial \Psi_e}{\partial X} \quad \text{at } X = 0, L$$

$$J_y = -\frac{2Cm}{1+Cm} \frac{\partial \Psi_e}{\partial Y} \quad \text{at } Y = 0, L$$

$$J_z = -\frac{2Cm}{1+Cm} \frac{\partial \Psi_e}{\partial Z} \quad \text{at } Z = 0, L$$

where $Cm\ (=\sigma_w/\sigma)$ represents the electro-conductivity of the wall divided by that of fluid. The outer side of the wall was assumed to be electrically insulated as follows:

$$J_x = 0 \quad \text{at } X = -0.0962L, 1.0962L$$

$$J_y = 0 \quad \text{at } Y = -0.0962L, 1.0962L$$

$$J_z = 0 \quad \text{at } Z = -0.0962L, 1.0962L.$$

5. DEFINITION OF THE AVERAGE NUSSELT NUMBER

The average Nusselt number was computed as a ratio of the total heat flux divided by the conductive heat flux under the same temperature boundary condition as the convective heat transfer case as follows:

$$Nu = \frac{\text{total heat flux}}{\text{conductive heat flux}} = \int_0^L \int_0^L \left(\frac{\partial T_{conv}}{\partial X}\right)_{X=0} dY dZ \Big/ \int_0^L \int_0^L \left(\frac{\partial T_{cond}}{\partial X}\right)_{X=0} dY dZ. \tag{8}$$

Where, T_{conv} represents convective temperature which can be obtained by solving the simultaneous equations in Section 2. T_{cond} represents conductive temperature obtained by solving the energy equation excluding the convective terms.

6. COMPUTED RESULTS AND DISCUSSION

The computational parameters and the resultant average Nusselt numbers are listed in Table 2. The average Nusselt number decreases with Cm under the X-directional magnetic field and agrees with the pre-

Table 2. The computational parameters and the resultant average Nusselt numbers

	Ra	Pr	Ha	Cm	Nu for X-mag.	Nu for Y-mag.
Present work	10^5	0.025	0	—	2.789	2.789
	10^5	0.025	100	0	1.596	2.728
				0.01	1.592	2.720
				0.1	1.555	2.646
				1	1.396	2.180
				10	1.262	1.540
				100	1.238	1.393
				∞	1.235	1.363
Ref. [3]	10^5	0.025	100	∞	1.232	1.071

vious simplified results [3] shown in the last row. On the other hand under the Y-directional magnetic field, it does not agree with the simplified solution. This means that some amount of electric field is induced in the fluid even for the perfectly electro-conducting walls ($Cm = \infty$) under the Y-directional magnetic field.

Figure 3 shows the transient responses of the average Nusselt number on the heated wall after a step input of (a) the X- or (b) the Y-directional magnetic fields at $Ha = 100$, $Ra = 10^5$ and $Pr = 0.025$. In the present work, only $Ha = 100$ was considered as a representative case of the magnetic field. For the X-directional magnetic field, the effect of Cm is not strong. On the contrary, for the Y-directional magnetic field the average Nusselt number changes extensively depending on Cm.

These average Nusselt numbers are plotted vs Cm on a semi-logarithmic graph in Fig. 4. When the electro-conductivity of the wall is small, i.e., Cm is small, the average Nusselt numbers differ extensively dependent on the direction of the magnetic field. The Y-directional magnetic field is far less effective to suppress the natural convection of liquid metal than the X-directional one. On the other hand, when the electro-conductivity of the wall becomes large, i.e., Cm is large, the suppressing effect becomes large independent of the direction of the magnetic field.

Figure 5 shows the perspective views of velocity vectors for the X-directional magnetic field at $Ra = 10^5$, $Ha = 100$ and $Pr = 0.025$. These vectors are drawn not only for fluid region but also for wall region. At $Cm = 0$, those velocity vectors near the side walls are larger than those in the central region. At $Cm = \infty$, the magnitude of velocity vectors are almost equal everywhere.

Figure 6 shows the perspective views of velocity vectors for the Y-directional magnetic field at

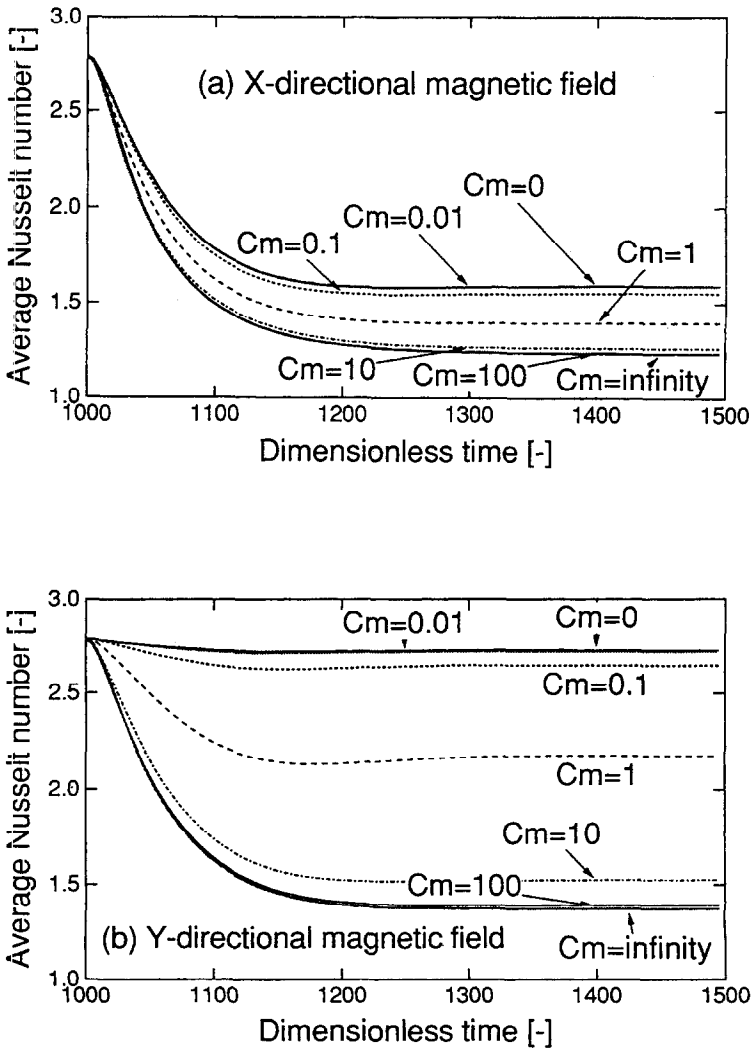

Fig. 3. Transient responses of the average Nusselt number on the heated wall for the effect of electro-conductivity ratio at $Ha = 100$, $Ra = 10^5$ and $Pr = 0.025$. (a) X-directional magnetic field. (b) Y-directional magnetic field.

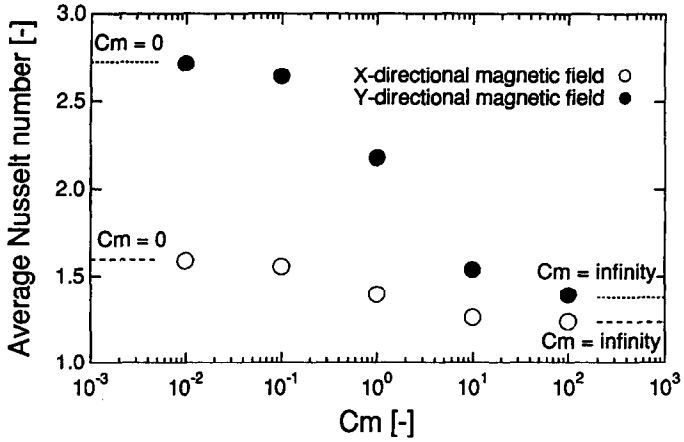

Fig. 4. The effect of electro-conductivity of the wall at $Ha = 100$, $Ra = 10^5$ and $Pr = 0.025$.

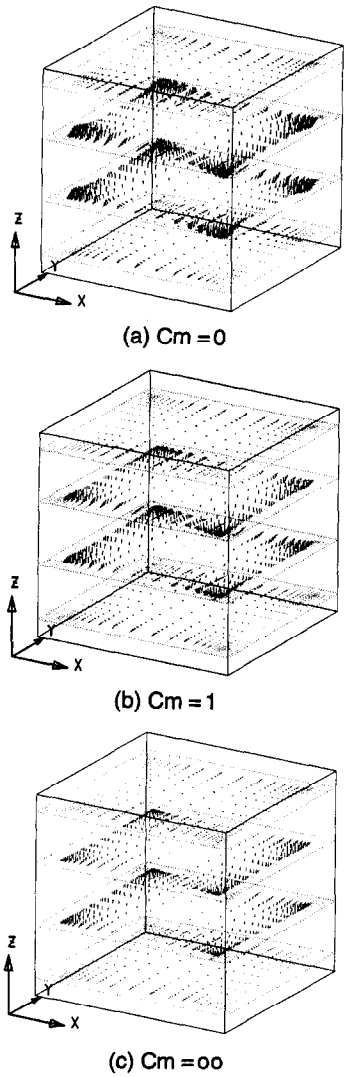

Fig. 5. Perspective views of velocity vectors for the X-directional magnetic field at $Ra = 10^5$, $Ha = 100$ and $Pr = 0.025$. Both fluid and surrounding wall regions are presented.

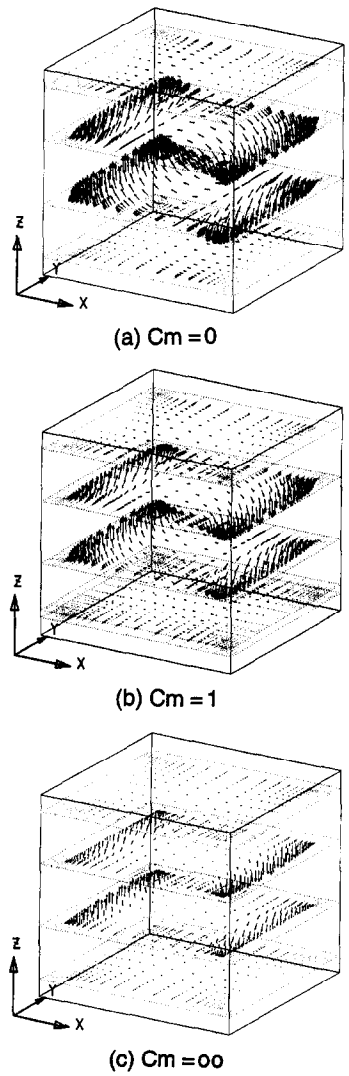

Fig. 6. Perspective views of velocity vectors for the Y-directional magnetic field at $Ra = 10^5$, $Ha = 100$ and $Pr = 0.025$.

$Ra = 10^5$, $Ha = 100$ and $Pr = 0.025$. The velocity vectors are drawn in the same scale as in the X-directional magnetic field. The velocity vectors are much larger than those in Fig. 5. This suggests that the suppression is much weaker in the Y-directional magnetic field for $Cm = 0$. The flow is drastically suppressed with the increase in Cm. In the Y-directional magnetic field, the magnetic suppression increases seriously with the increase in Cm, the electro-conductivity of the wall.

In this paper, numerical calculations were not carried out for the Z-directional magnetic field in general, because the suppressing effect of the Z-directional magnetic field is almost equivalent to the X-directional magnetic field [1–3]. Under the X-directional magnetic field, vertical velocity component is suppressed by the Lorentz force, and horizontal velocity component is suppressed under the Z-directional magnetic field almost equally. Hence, the suppressing effect on the circulating flow is almost identical between these two magnetic fields. Figure 7 shows those computed (a) in the X- and (b) in the Z-directional magnetic field, otherwise the same conditions.

Subsequent discussion is for the reasoning why the suppressing effect differs so much between the X- and the Y-directional magnetic field. To account for the reason, the magnitudes of the electric current density due to the electric field $\mathbf{E}$ and the vector product $\mathbf{U} \times \mathbf{B}$ are evaluated. The following figures of vectors are drawn in the same scale.

Figure 8 shows the electric current density due to the electric field $\mathbf{E}$ in (a)–(c) and the vector product $\mathbf{U} \times \mathbf{B}$ in (d)–(f) for the X-directional magnetic field at $Z = 0.4339L$. Those in the wall are given by $Cm\mathbf{E}$. At $Cm = 0$ (perfectly electro-insulated wall), the electric current density vectors due to electric field are zero in the wall region. The electric current density in the fluid decreases with the increase in Cm, while that in the wall increases with the increase in Cm. At $Cm = \infty$ (perfectly electro-conducting wall), the electric current density due to electric field almost vanishes in the fluid. Due to the heated and cooled walls, the ascending and descending flows induce the vector product $\mathbf{U} \times \mathbf{B}$ whose direction is in the Y-direction near the heated and cooled walls. At $Cm = 0$, the vectors at four corners are larger than any other portions, because velocity vectors near the side walls are larger as shown in Fig. 5.

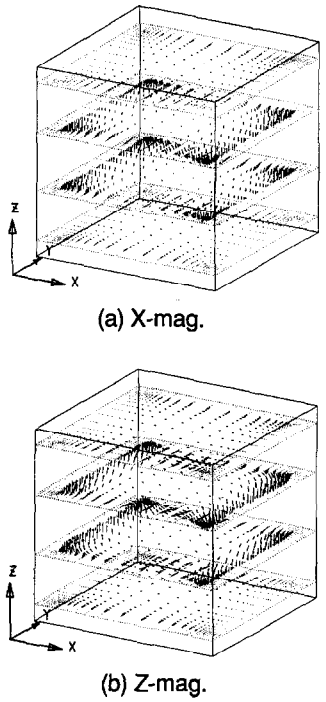

Fig. 7. Comparison between the X- and Z-directional magnetic field at $Cm = 1$, $Ha = 100$, $Ra = 10^5$ and $Pr = 0.025$. (a) The X-directional magnetic field and $Nu = 1.396$. (b) The Z-directional magnetic field and $Nu = 1.416$.

Figure 9 shows the total electric current density vectors $\mathbf{J} = \mathbf{E} + \mathbf{U} \times \mathbf{B}$ for the X-directional magnetic field at $Z = 0.4339L$. For example, Fig. 8(b) and Fig. 8(e) give Fig. 9(d) for $Cm = 1$. In the wall region, the electric current density is given by equation (5) $\mathbf{J} = Cm\mathbf{E}$. The electric current density is continuous between the wall and the fluid regions. In the fluid region, the vector product $\mathbf{U} \times \mathbf{B}$ is dominant only in the Y-direction but summation with the electric current density due to electric field $\mathbf{E}$ gives the X-directional electric current density. Hence, a large clockwise circulation is resulted in the fluid region. Besides, four small anticlockwise circulations can be seen at

Table 3. Physical properties of Ga (310 K) [2]

Property	Value	Unit
Density	6.091×10^3	$\mathrm{kg\,m^{-3}}$
Viscosity	1.902×10^{-3}	$\mathrm{Pa \cdot s}$
Specific heat	3.976×10^2	$\mathrm{J\,(kg \cdot K)^{-1}}$
Thermal conductivity	3.149×10^1	$\mathrm{W\,(m \cdot K)^{-1}}$
Volumetric coefficient of thermal expansion	1.267×10^{-4}	$\mathrm{K^{-1}}$
Electric conductivity (313.15 K)	3.85×10^6	$\mathrm{(\Omega \cdot m)^{-1}}$
Magnetic permeability	$4\pi \times 10^{-7}$	$\mathrm{H\,m^{-1}}$
Melting point	302.93	K

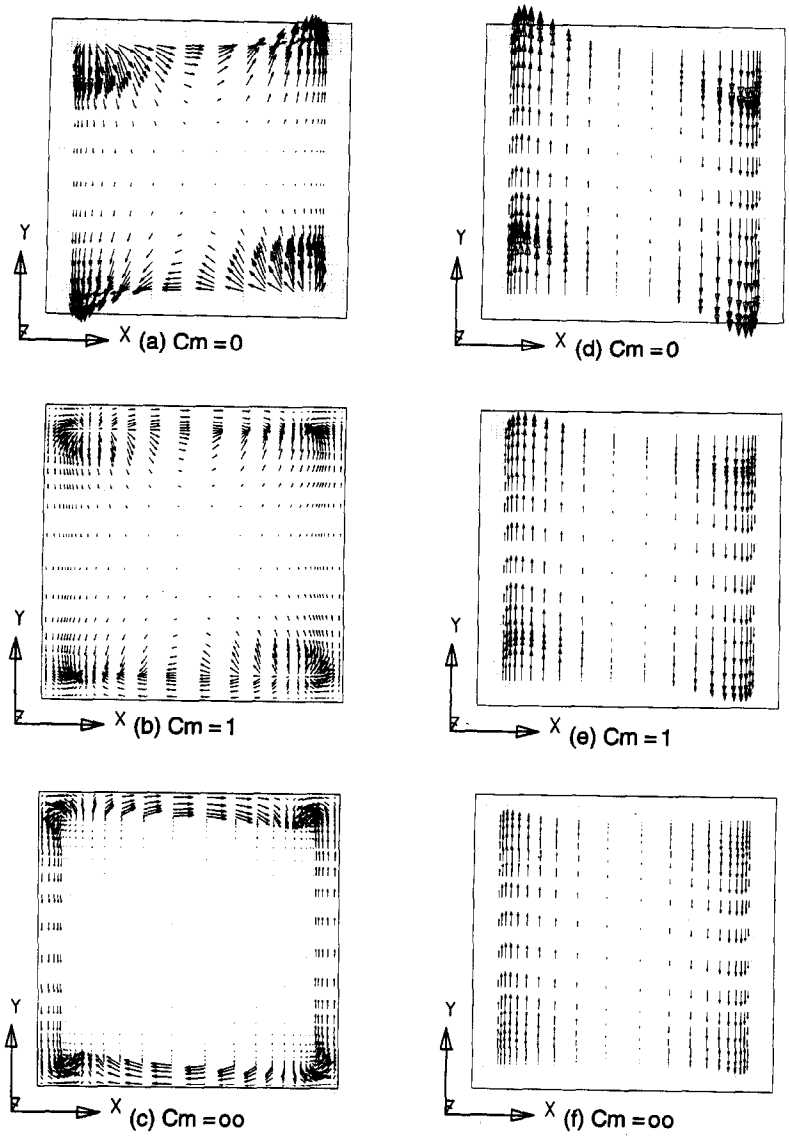

Fig. 8. Electric current density vectors due to electric field **E** (left hand side) and vector product $\mathbf{U} \times \mathbf{B}$ (right hand side) for the X-directional magnetic field at $Z = 0.4339L$, $Ra = 10^5$, $Ha = 100$ and $Pr = 0.025$ in the fluid region. In the wall region, $\mathbf{J} = Cm\mathbf{E}$.

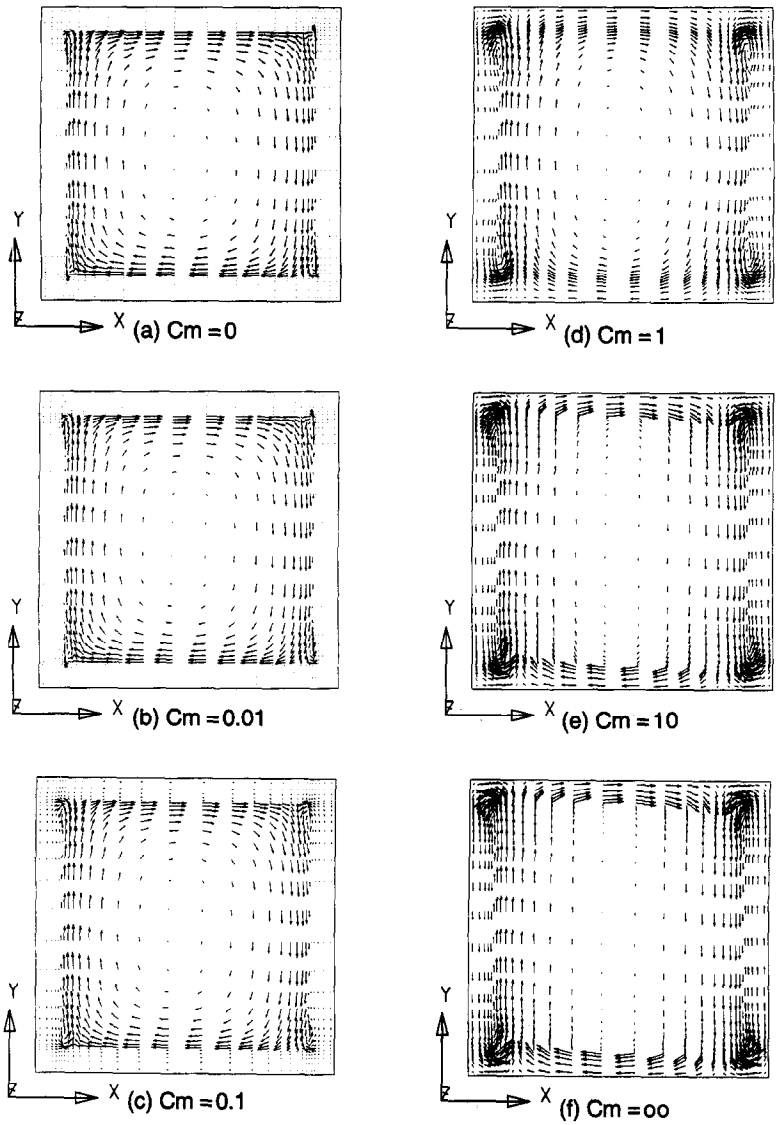

Fig. 9. Total electric current density vectors $\mathbf{J} = \mathbf{E} + \mathbf{U} \times \mathbf{B}$ for the X-directional magnetic field at $Z = 0.4339L$, $Ra = 10^5$, $Ha = 100$ and $Pr = 0.025$ in the fluid region. In the wall region, $\mathbf{J} = Cm\mathbf{E}$.

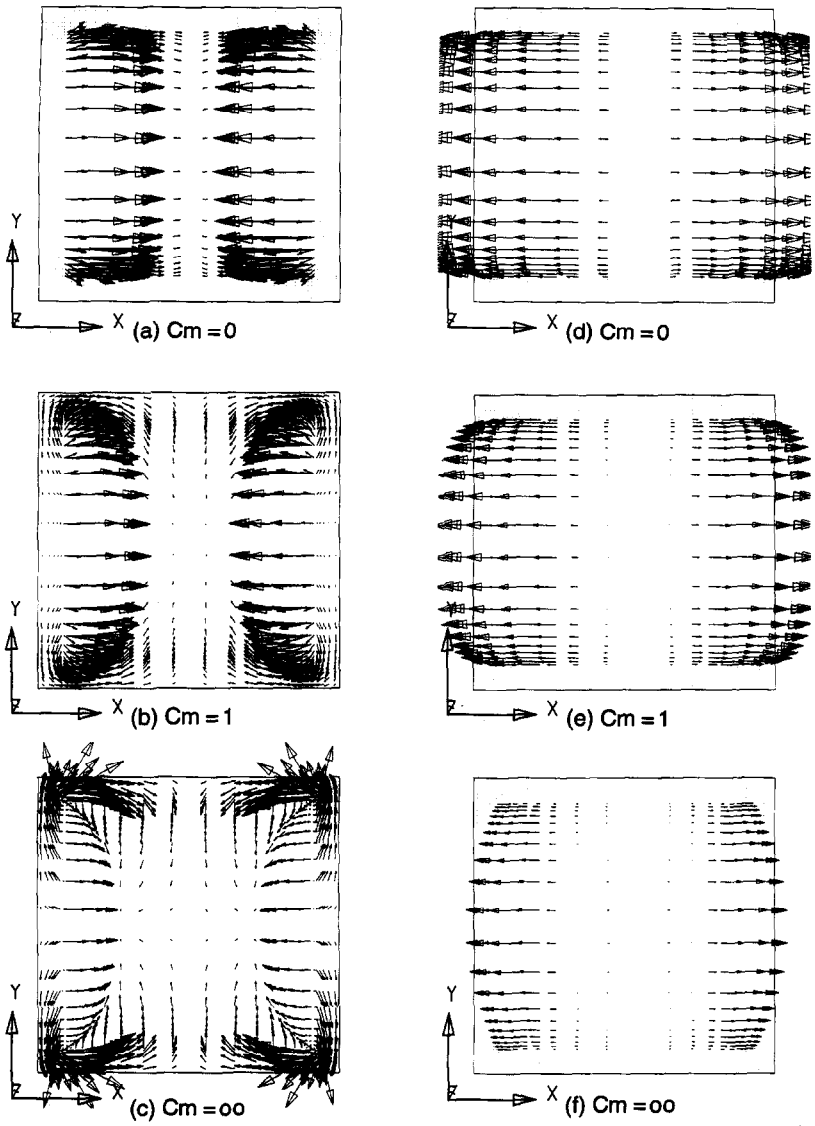

Fig. 10. Electric current density vectors due to electric field **E** (left hand side) and vector product $\mathbf{U} \times \mathbf{B}$ (right hand side) for the Y-directional magnetic field at $Z = 0.4339L$, $Ra = 10^5$, $Ha = 100$ and $Pr = 0.025$ in the fluid region. In the wall region, $\mathbf{J} = Cm\mathbf{E}$.

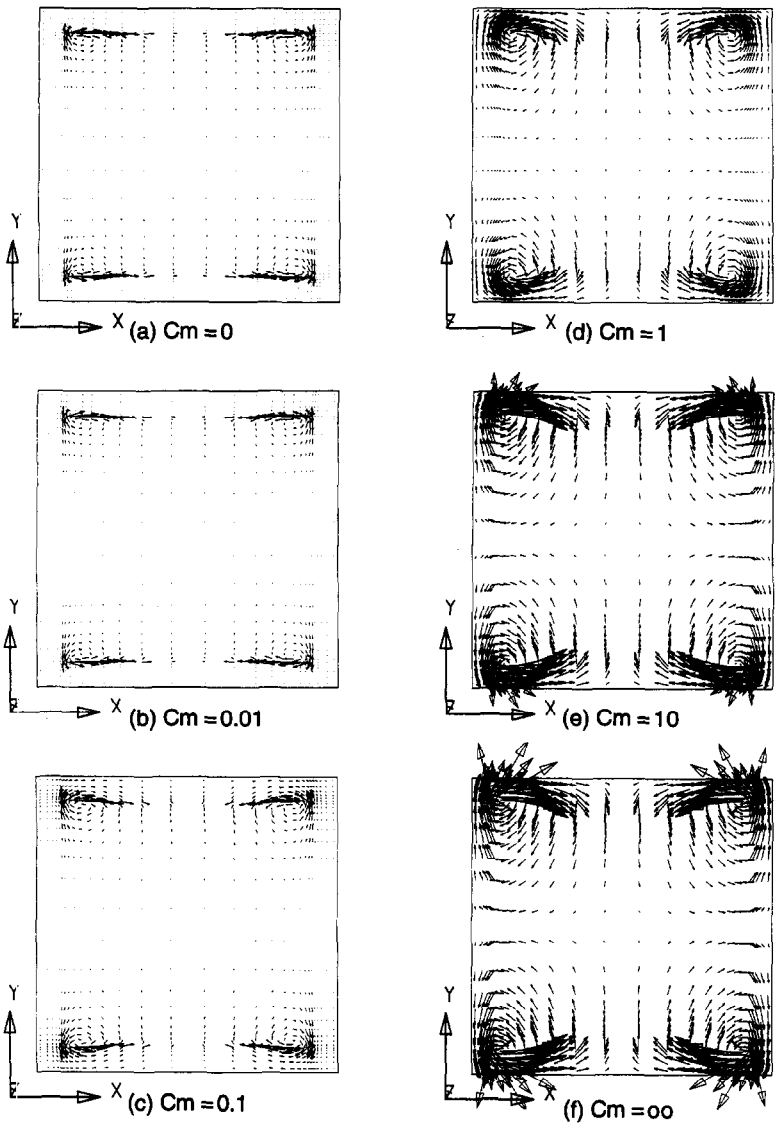

Fig. 11. Total electric current density vectors $\mathbf{J} = \mathbf{E} + \mathbf{U} \times \mathbf{B}$ for the Y-directional magnetic field at $Z = 0.4339L$, $Ra = 10^5$, $Ha = 100$ and $Pr = 0.025$ in the fluid region. In the wall region, $\mathbf{J} = Cm\mathbf{E}$.

four corners. At $Cm \geqslant 10$, since the electric field **E** almost vanishes in the fluid, the electric current density **J** is mostly contributed by the vector product $\mathbf{U} \times \mathbf{B}$ in the fluid region.

Figure 10(a)–(c) shows the electric current density vectors due to electric field **E** and the vector product $\mathbf{U} \times \mathbf{B}$ in Fig. 10(d)–(f) for the Y-directional magnetic field at $Z = 0.4339L$. Compared to the X-directional magnetic field, the Y-directional magnetic field has larger magnitude of the electric current density for any Cm values. Even at $Cm = \infty$, some amount of the electric current density is computed in the fluid region, although those magnitude at $Cm = \infty$ are much smaller than those at $Cm = 0$. Most of the electric current density vectors are in the X-direction due to the main circulation of the natural convection.

Figure 11 shows the summation of **E** and $\mathbf{U} \times \mathbf{B}$ to give the total electric current density vectors for the Y-directional magnetic field at $Z = 0.4339L$. At $Cm \leqslant 0.1$, the electric field **E** cancels out with the vector product $\mathbf{U} \times \mathbf{B}$ with an inverse sign and the electric current density **J** becomes almost zero except near the side boundaries ($Y = 0$ and L). The Lorentz force becomes quite small for small Cm region. At $Cm = 1$, electric current density **J** becomes rather large both in the fluid and wall regions. The larger amount of the electric current density **J** in the fluid region works to suppress the convection. At $Cm \geqslant 10$, the electric current density **J** becomes much larger and the suppression due to the Lorentz force becomes remarkable. For the high value of Cm, the electric current due to terms **E** and $\mathbf{U} \times \mathbf{B}$ does not cancel out each other and the suppressing effect becomes effective even for the Y-directional magnetic field.

7. CONVERSION INTO DIMENSIONAL VALUES

The cubic enclosure was assumed to be filled with gallium whose Pr number is 0.025. Physical properties of Ga [2] are listed in Table 3. When the internal length of the cubic enclosure is 64 mm, $Ha = 100$ and $Ra = 10^5$ are almost equivalent to 0.035 T (magnetic flux density) and 1.2 K (temperature difference between hot and cold walls), respectively. The electro-conductivity ratio of the wall, $Cm = 15$, 2.7 and 0.24 correspond to copper, iron and Nichrome, respectively.

8. CONCLUSIONS

The natural convection of liquid metal in a cubical enclosure was numerically studied for the electro-conductivities of the wall from zero to infinity under the X- or Y-directional magnetic fields. Under the X-directional magnetic field, induced electric field **E** and $\mathbf{U} \times \mathbf{B}$ term gave a circulating electric current and large Lorentz force was resulted for any values of the electro-conductivity of the wall. Under the Y-directional magnetic field when the electro-conductivity of the wall was small, the natural convection of liquid metal was suppressed slightly because the vector product $\mathbf{U} \times \mathbf{B}$ was almost canceled out by the induced electric field **E**. The effect of magnetic suppression differed enormously between the X- and Y-directional magnetic fields when the dimensionless electro-conductivity of the wall is less than unity. However, with the increase in the electro-conductivity of the wall, the electric current density in the fluid increases both under the X- and Y-directional magnetic fields and the Lorentz force becomes effective irrespective of the direction of the magnetic field.

REFERENCES

1. Ozoe, H. and Okada, K., The effect of the direction of the external magnetic field on the three-dimensional natural convection in a cubical enclosure. *International Journal of Heat and Mass Transfer*, 1989, **32**, 1939–1954.
2. Okada, K. and Ozoe, H., Experimental heat transfer rates of natural convection of molten gallium suppressed under an external magnetic field in either the X-, Y-, or Z-direction. *Journal of Heat Transfer*, 1992, **114**, 107–114.
3. Tagawa, T. and Ozoe, H., Three-dimensional numerical analyses of natural convection of liquid metal in a cube with electro-conducting walls under an external magnetic field either in the X-, Y-, or Z-directions. *The 14th International Riga Conference on Magnetohydrodynamics*. Jurmala, Latvia, 1995.
4. Hirt, C. W., Nichols, B. D. and Romero, N. C., *Los Alamos Scientific Laboratory*, 1975, **La-5852**.
5. Tagawa, T. and Ozoe, H., Effect of Prandtl number and computational schemes on the oscillatory natural convection in an enclosure. *Numerical Heat Transfer, Part A*, 1996, **30**, 271–282.